Published in final edited form as:
J Mol Cell Cardiol. 2012 August ; 53(2): 176–186. doi:10.1016/j.yjmcc.2012.05.001.

$PKC\beta_{II}$ Modulation of Myocyte Contractile Performance

Hyosook Hwang[1,*], **Dustin A Robinson**[1], **Tamara K Stevenson**[1], **Helen C Wu**[1], **Sarah E Kampert**[2], **Francis D Pagani**[1], **D. Brad Dyke**[3], **Jody L Martin**[4], **Sakthival Sadayappan**[5], **Sharlene M Day**[3], and **Margaret V Westfall**[1]

[1]Dept. of Surgery, Cardiac Surgery Section, University of Michigan, Ann Arbor, MI 48109

[2]Program in Cellular and Molecular Biology, University of Michigan, Ann Arbor, MI 48109

[3]Cardiovascular Division, Department of Internal Medicine, University of Michigan, Ann Arbor, MI 48109

[4]Dept. of Medicine/Division of Cardiology, Loyola University of Chicago, Maywood, IL 60153

[5]Dept. of Physiology, Loyola University of Chicago, Maywood, IL 60153

Abstract

Significant up-regulation of the protein kinase $C\beta_{II}$ ($PKC\beta_{II}$) develops during heart failure and yet divergent functional outcomes are reported in animal models. The goal here is to investigate $PKC\beta_{II}$ modulation of contractile function and gain insights into downstream targets in adult cardiac myocytes. Increased $PKC\beta_{II}$ protein expression and phosphorylation developed after gene transfer into adult myocytes while expression remained undetectable in controls. The $PKC\beta_{II}$ was distributed in a perinuclear pattern and this expression resulted in diminished rates and amplitude of shortening and re-lengthening compared to controls and myocytes expressing dominant negative $PKC\beta_{II}$ (PKCβDN). Similar decreases were observed in the Ca^{2+} transient and the Ca^{2+} decay rate slowed in response to caffeine in $PKC\beta_{II}$-expressing myocytes. Parallel phosphorylation studies indicated $PKC\beta_{II}$ targets phosphatase activity to reduce phospholamban (PLB) phosphorylation at residue Thr17 (pThr17-PLB). The PKCβ inhibitor, LY379196 (LY) restored pThr17-PLB to control levels. In contrast, myofilament protein phosphorylation was enhanced by $PKC\beta_{II}$ expression, and individually, LY and the phosphatase inhibitor, calyculin A each failed to block this response. Further work showed $PKC\beta_{II}$ increased Ca^{2+}- activated, calmodulin-dependent kinase IIδ (CaMKIIδ) expression and enhanced both CaMKIIδ and protein kinase D (PKD) phosphorylation. Phosphorylation of both signaling targets also was resistant to acute inhibition by LY. These later results provide evidence $PKC\beta_{II}$ modulates contractile function via intermediate downstream pathway(s) in cardiac myocytes.

Address for Correspondence: Margaret V Westfall, 263S Building 26 NCRC, 2800 Plymouth Road, University of Michigan, Ann Arbor, MI 48109-2800, wfall@umich.edu, Phone: 734-615-8911, Fax: 734-763-0323.
*Current address: Dept. of Physiology, Medical Research Building 320, University of Arizona College of Medicine, Tucson, AZ 85724

DISCLOSURES
None

Keywords

Protein kinase C; cardiac myocyte; contractile function; gene transfer

INTRODUCTION

Protein kinase C (PKC) modulates cardiac function and there is evidence isoforms of PKC target proteins in Ca^{2+} cycling and the contractile apparatus of myocytes [1, 2]. Increased cardiac PKC isoform expression is associated with contractile dysfunction and a variety of pathological conditions [2–5]. However, it remains difficult to identify the role played by each PKC isoform in modulating contractile function or dysfunction. In particular, it is known that $PKC\beta_{II}$ expression and activity increases during the development of cardiac hypertrophy and the progression to heart failure [3,6–8]. While up-regulation of this isoform is linked to cardiac dysfunction in humans [3,7,8], the functional role played by $PKC\beta_{II}$ in modulating contractile function remains uncertain.

In earlier work with transgenic mice expressing $PKC\beta_{II}$, cardiomyocyte contractility increased in one and decreased in a second animal model [4,9]. More recently, investigators reported little difference in the ventricular response to ischemia or pressure overload after PKCβ knockout [10]. The explanation for these different phenotypes is not well understood, and may result from a number of possibilities. For example, there may be divergent localization of $PKC\beta_{II}$ in response to up-regulation, as the wildtype isoform is expressed in one transgenic model while a constitutively active form is utilized in the other [4,9]. Differences in the developmental expression and/or compensatory adaptations to load also may contribute to the divergent functional outcomes in these models [4]. Thus, questions remain about the role $PKC\beta_{II}$ plays in modulating contractile function in cardiac myocytes.

One step toward understanding $PKC\beta_{II}$ modulation of function is to identify the targets for phosphorylation. Biochemical and animal model studies identified several targets for $PKC\beta_{II}$, including proteins with a direct role in Ca^{2+} handling and myofilament proteins involved in contractile function. For example, *in vitro* activation of $PKC\beta_{II}$ phosphorylated the regulatory protein, cardiac troponin I (cTnI) [11]. Enhanced cTnI phosphorylation also developed in wildtype $PKC\beta_{II}$ transgenic mouse hearts with impaired contractile performance [9]. Additional biochemical studies indicated $PKC\beta_{II}$ activation phosphorylates the sarcoplasmic reticulum (SR) protein, phospholamban (PLB) which modulates sarcoplasmic reticulum (SR) Ca^{2+} uptake via the SR Ca^{2+}-ATPase, SERCA2A [12]. PKCα, the other major classical isoform expressed in mammalian heart also modulates PLB phosphorylation [2]. Given PKC-α and -β both increase in failing hearts [3,7,13], the influence of $PKC\beta_{II}$ on myofilament and Ca^{2+} cycling targets continues to be of interest.

Efficient gene expression in intact cardiac myocytes can be used to acutely increase expression using adenoviral-mediated gene transfer. This approach is utilized here to gain insights into the role of $PKC\beta_{II}$ in modulating cardiac myocyte contractile function, and serves as an important adjunct to earlier findings in animal models by determining the acute influence of $PKC\beta_{II}$ up-regulation on cellular contractile function. In addition, the present study is designed to determine whether the PKC targets identified in earlier biochemical studies [14–16] are phosphorylated in intact cells and correlates with the functional response. Our study also set out to determine whether this isoform targets other signaling pathways in intact myocytes.

METHODS

Adenoviral constructs

Recombinant $PKC\beta_{II}$ and dominant negative $PKC\beta_{II}$ (PKCβDN) adenoviruses were kind gifts from Jeffery Molkentin (Cincinnati Children's Hospital) and were originally generated by Ohba et al. [17,18]. PKCβ was cloned into the Kpn1/Xba1 site of pEGFP-1 (Clontech Laboratories, Inc, Mountain View, CA), subcloned into the pACCMVpLpA shuttle plasmid, and then co-transfected with pJM17 in HEK 293 cells to generate the PKCβGFP recombinant adenovirus. High titer stocks of each viral construct were prepared as described earlier (19).

Myocyte isolation and gene transfer

Adult rat cardiac myocytes were isolated as described in earlier studies [19]. Briefly, myocytes were isolated from heparinized rats with collagenase and hyaluronidase to digest the heart, and then cells were made Ca^{2+} tolerant over 15 min. Isolated myocytes were plated on laminin-coated coverslips for 2 hours in DMEM plus penicillin (50 U/ml), streptomycin (50 μg/ml; P/S), and 5% FBS. Two hours later, gene transfer was carried out with high titer $PKC\beta_{II}$, PKCβDN or PKCβGFP (10 MOI) recombinant adenovirus [19]. At this MOI, ~80% of cardiac myocytes expressed GFP 2 days after gene transfer (unpublished results). Myocytes were electrically paced in M199 plus P/S media 24 hrs after plating, with subsequent media changes every 12 hrs [20].

A similar protocol was used to isolate adult myocytes from New Zealand male rabbits (2.2–2.6 kg) with the following modifications. Isolated hearts were immersed in an ice cold 50:50 mixture of Joklik-modified MEM (JMEM) and Hank's Balanced Salt Solution plus 15 mM HEPES and P/S. Hearts were initially perfused with Ca^{2+}-free DMEM plus 15 mM HEPES and P/S at 37°C, followed by DMEM supplemented with 10 mM HEPES, P/S, collagenase (250 U/ml), and hyaluronidase (0.1 mg/ml) for 10 min, Protease type XIV (0.2 mg/ml) was added to the perfusate for an additional 15 min. Isolated myocytes were made Ca^{2+} tolerant in DMEM plus 10 mM HEPES, 2.5 mg/ml BSA, P/S and 1.25 μM $CaCl_2$, with re-addition of Ca^{2+} to a final concentration of 1.80 mM over 1 hr, and then plated in DMEM supplemented with 5% FBS and P/S. Two hours later, gene transfer was carried out with recombinant adenovirus diluted in serum free DMEM plus P/S for 1 hr, followed by the addition of fresh serum-free media. Myocytes were then cultured in M199 plus P/S within 24 hrs after plating. All animal procedures followed the guidelines and were approved by the University Committee on Use and Care of Animals at the University of Michigan.

Contractile function and Ca^{2+} transient measurements

Sarcomere shortening was measured in isolated myocytes 2–3 days after gene transfer, as described previously [21]. Briefly, coverslips were transferred to a 37°C temperature-controlled chamber, perfused with M199 plus P/S and paced at 0.2 Hz. Sarcomere shortening under basal conditions was measured using video-based microscope camera system (Ionoptix, Beverly, MA). Resting sarcomere length, peak shortening amplitude, shortening and re-lengthening rate, and time to 50% of peak amplitude ($TTP_{50\%}$) plus time to 25%, 50%, and 75% re-lengthening ($TTR_{25\%}$, $TTR_{50\%}$, and $TTR_{75\%}$) were determined for each myocyte. Calcium transients and sarcomere shortening were measured simultaneously in a subgroup of myocytes. These cells were loaded with Fura-2AM, as described earlier [21]. Signal averaged measurements of resting and peak Fura-2 ratios, the rates of Ca^{2+} rise and Ca^{2+} decay, and time to 50 and 75% decay ($TTD_{50\%}$, $TTD_{75\%}$) along with the sarcomere shortening measurements described above were collected from each myocyte.

Western Analysis

PKCβ expression and phosphorylation in myocytes were measured by Western analysis after gene transfer. Myocyte proteins were separated with 12% SDS-PAGE, as described earlier [20,21]. Separated protein bands were transferred onto PVDF membrane for 2000 V-hours, and expression detected on milk-blocked membranes using $PKC\beta_{II}$ primary antibody (Ab) (1:400; BD Biosciences, San Jose, CA). Anti-phospho-PKCα/β antibody (1:1000; Cell Signaling Technology, Inc, Danvers, MA) was used to measure phospho-PKC on BSA-blocked membranes. Both primary antibodies were detected with horseradish peroxidase-conjugated secondary antibodies and enhanced chemiluminescence. Quantitative analysis of protein expression on blots was determined with Quantity One software and normalized to actin expression (5C5; Sigma) and/or a silver-stained band on the SDS-PAGE.

$PKC\beta_{II}$ expression was assessed in tissue homogenates from failing human ventricular heart samples. Biopsy samples from non-failing donor hearts (non-failing; n=3) were compared to discarded explant tissue collected at the time of ventricular assist device (VAD) implantation in 15 patients with heart failure (n=15; 3 female, 12 male; 13 Caucasian, 2 African-American, Mean+SEM for age = 41±3 yr; ejection fraction = 11±1.2%, time from initial diagnosis to VAD implantation: 2.7±0.9 yr). All samples were frozen in liquid N_2 at the time of explant and stored at −80°C. Homogenates were prepared from tissue ground to a powder in liquid N_2 and then resuspended in sample buffer. Protein concentrations were determined for each sample prior to protein separation and Western detection of $PKC\beta_{II}$ (1:200; C-18; Santa Cruz Biotechnology, Santa Cruz, CA) by ECL. The protocol used to procure human heart tissue is approved by the University of Michigan Internal Review Board and Gift of Life – Michigan.

Western blot analysis also was used to detect expression and phosphorylation of downstream targets. For phosphorylation studies, media was replaced with fresh M199 + P/S to study basal phosphorylation, or media containing either 30 nM LY379196 (LY; ref 22; kind gift of C Vlahos, Eli Lilly, Indianapolis, IN) or 10 nM calyculin A (CalA) for 10 or 60 min. Then, myocytes were collected in ice-cold sample buffer and immediately stored at −80°C until proteins were separated by SDS-PAGE. Primary antibodies and dilutions used to detect each protein were: phospholamban (PLB; 1:1000; Millipore, Billerica, MA), phospho-PLB (pSer16-PLB, 1:1000 Millipore and pThr17-PLB; 1:5000; Badrilla, Leeds, UK), phospho-extracellular regulated kinase 1/2 (pERK1/2; 1:1000; Cell Signaling Tech, Beverly, MA), phospho-Ser23/24cTnI (pSer23/24-cTnI, Cell Signaling Tech), TnI (1:5000; MAB1691; Cell Signaling Tech), Ca^{2+}/calmodulin kinase IIδ (CaMKIIδ, 1:500; R&D Systems, Minneapolis, MN), phospho-Ser286CaMKIIδ (pCaMKIIδ; 1:500, ProMega, Madison, WI), protein kinase D (PKD; 1:1000, Cell Signaling, Inc), phospho-PKD (p-PKD; 1:1000, Cell Signaling, Inc), cardiac myosin binding protein C (cMyBP-C; pan) and phosphorylated cMyBP-C (Ser273, Ser282, and Ser302; 23), and SERCA2A (1:2000; Santa Cruz Biotechnology). An Odyssey infrared system was used to detect PLB, SERCA2A, cTnI, and all antibodies for MyBP-C with AlexaFluor700 or AlexaFluor800 secondary antibodies (1:5000; Invitrogen, Grand Island, NY). Horseradish peroxidase-conjugated secondary antibodies were used to detect pERK1/2, pSer23/24cTnI, pSer16PLB-Ser16, pThr17PLB, CaMKIIδ, pCaMKIIδ, PKD and pPKD by enhanced chemiluminescence. Protein expression on Western blots is expressed relative to antibody detection of actin on the same blot or a silver-stained portion of the gel and then normalized to expression in 2 day controls (control expression = 1.0). Expression of the phosphorylated/total protein ratio determined by Western analysis also was normalized to the ratio detected in 2 day controls. Myosin heavy chain (MHC) isoform composition was determined on silver (Ag)-stained 8% SDS-PAGE gels, as described earlier (24).

Immunofluorescence

PKCβ localization was analyzed by indirect immunohistochemistry in paraformaldehyde-fixed myocytes, as described previously [19]. Primary $PKC\beta_{II}$ antibody (BD Biosciences) and fluorescein isothiocyanate- (FITC, Invitrogen) conjugated goat anti-mouse secondary antibody were used to label myocytes 2 days after gene transfer. Live cell imaging of PKCβGFP was performed using a Nikon TiU inverted fluorescent microscope equipped with DS-Fi1 5 megapixel digital imaging 2–3 days after gene transfer.

Phosphodetection after radiolabeling with ^{32}P

Phosphorylation also was analyzed in myocytes labeled with ^{32}P-orthophosphate (100 μCi) for 2 hrs [25] and then transferred to M199 media with or without 30 nM LY for 10 min. Phosphorylation was terminated in ice-cold relaxing solution (RS; 7 mM EGTA, 20 mM imidazole, 1 mM free Mg^{2+}, 14.5 mM creatine phosphate, and 4 mM MgATP with KCl added to yield an ionic strength of 180 mM, pH 7.00) and myocytes were immediately collected in ice-cold sample buffer (15% glycerol, 1% SDS, 62.5 mM Tris (pH 6.8), 0.01% bromophenol blue, 15 mM DTT, 1 mM leupeptin). Proteins from each sample were separated on 12% SDS-PAGE gels, silver stained and dried overnight. Radioactive phosphate incorporation was measured with a phosphor-imager (Bio-Rad, Hercules, CA) and bands were quantified using Quantity One software. Proteins were identified based on their migration relative to molecular weight markers. Phosphorylation is expressed relative to a silver (Ag)-stained band on the SDS-PAGE gel and normalized to control levels.

Statistical analysis

Results are expressed as mean ± SEM. A one-way analysis of variance (ANOVA) and post-hoc Newman-Keuls tests were used to analyze protein expression and indices of myocyte contractile function (resting length, peak amplitude, shortening and re-lengthening rate, TTP and TTR measurements) and the Ca^{2+} transient (basal ratio, peak Ca^{2+}, TTD, tau, and rate of rise and decay of Ca^{2+}), with statistical significance set at $p<0.05$ (*). Phosphorylation detected with ^{32}P-labeling in $PKC\beta_{II}$-expressing myocytes was compared to the control value set at 1.0 using a Student's T-test, with $p<0.05$ considered statistically significant.

RESULTS

Gene transfer and expression of $PKC\beta_{II}$ in adult myocytes

Temporal increases in $PKC\beta_{II}$ expression developed over 3 days after gene transfer into rat myocytes (Fig. 1A,B), while expression remained undetectable over the same time interval in controls. This level of expression in myocytes is comparable to levels reported in earlier work in transgenic mice [26]. Further analysis showed $PKC\beta_{II}$ up-regulation did not cause changes in PKC α, δ, or ε expression (Fig. 1C, Table 1), which could independently influence contractile performance [2,27–29]. The increased $PKC\beta_{II}$ expression also produced a corresponding increase in classical PKC phosphorylation (Fig. 1D; Control, 0.2 ± 0.1 arbitrary unit; AU; $PKC\beta_{II}$, 2.2 ± 0.1 AU; n=12; *$p<0.05$). The up-regulation and phosphorylation of $PKC\beta_{II}$ are consistent with an increase in kinase activity [30], although commercial antibodies cannot distinguish between PKC-α (Thr638) and PKC-β (Thr641) phosphorylation. Comparable titers of PKCβDN also increased expression after gene transfer (Fig. 1A,B), with negligible changes in classical PKC phosphorylation (Fig. 1D). However, initial dominant negative expression sometimes lagged slightly behind the increase in $PKC\beta_{II}$ (Fig. 1B). Our studies in failing human hearts also verified there were similar increases in PKCβ up-regulation (Fig. 1E; 3, 8, 31).

Gene transfer-mediated changes in myosin heavy chain β composition

PKCβ_{II} expression has the potential to alter myofilament protein isoform expression, and causes a shift from α to βMHC gene expression in transgenic mice [26]. These changes are not observed in rat myocytes over 5–7 days in culture (24) and gel analysis confirmed MHC isoform expression remained comparable to controls after gene transfer (Fig. 1F; βMHC/total MHC: Control = 9.0±1.8%, n=8 hearts; PKCβ_{II} = 7.0±0.6%, n=8; $p > 0.05$).

Influence of PKCβ_{II} on myocyte contractile performance

Basal function—The impact of PKCβ_{II} and PKCβDN up-regulation on sarcomere shortening was then measured in intact, electrically paced adult rat myocytes. Two days after gene transfer of PKCβ_{II}, the amplitude (e.g. peak height) decreased and shortening rate slowed compared to controls. Resting sarcomere length, re-lengthening rate, $TTR_{25\%}$ and $TTR_{75\%}$ were not different among the 3 groups (Fig. 2A, B). Shortening and re-lengthening rates and the amplitude remained significantly depressed 3 days after gene transfer (Fig 2B right panel). A similar trend also began to develop within 1 day after gene transfer, although these changes were not statistically significant (Supplemental Fig. 1). At both day 2 and 3, peak shortening, and the rates of shortening and re-lengthening were not different between controls and myocytes expressing PKCβDN (Fig. 2). Collectively, these observations show PKCβ_{II} up-regulation negatively modulated rat myocyte shortening and re-lengthening, independent of resting length.

Expression and function in rabbit myocytes—To determine whether species differences influence PKCβ_{II} protein expression and/or modulation of contractile performance, additional functional studies were carried out using isolated adult rabbit myocytes. PKCβ_{II} and PKCβDN protein expression increased over time, with comparable increases 2 days after gene transfer into rabbit myocytes (Supp Fig. 2A). As with rat, the shortening rate decreased in rabbit myocytes with PKCβ_{II} up-regulation (Supp Fig. 2B). Although there was a trend for diminished shortening amplitude in myocytes expressing PKCβ_{II}, this difference was not statistically different from controls. Overall, the impact of up-regulation on contractile function was similar in rat and rabbit myocytes, and qualitative functional differences may be related to species differences.

Relationship between Ca^{2+} transient and contractile function—Rat myocytes were loaded with Fura-2AM to determine whether the Ca^{2+} transient contributed to diminished cellular function with PKCβ_{II} expression. In these studies, a decrease in the Ca^{2+} transient amplitude accompanied the PKCβ_{II}-induced reduction in peak shortening (Fig. 3). Comparable reductions in Ca^{2+} transient decay also developed with the slowed re-lengthening rate and longer $TTR_{75\%}$ for PKCβ_{II}- compared to controls or PKCβDN-expressing myocytes. PKCβ_{II} slowed shortening rate in these myocytes, and while the Ca^{2+} transient rate tended to decrease, this change was not significantly different from controls. In further studies, Ca^{2+} reuptake in response to caffeine was significantly slowed in PKCβ_{II}-expressing myocytes, while the amplitude of Ca^{2+} release was similar among cells from all three groups (Fig. 4). Together, these experiments show increased PKCβ_{II} expression correlates with changes in peak shortening, Ca^{2+} transient amplitude, and the re-lengthening and Ca^{2+} decay rates. The slowing of Ca^{2+} re-uptake by the SR likely contributes to the diminished decay rate.

PKCβ_{II} localization in cardiac myocytes—Our studies then turned to the PKCβ_{II} localization pattern in myocytes. Immunohistochemical staining and confocal imaging showed a peri-nuclear distribution of PKCβ_{II} 2 days after gene transfer along with a less intense, but consistent punctate pattern (Fig. 5A). This isoform remained non-detectable in

controls (Fig. 5B). Fluorescence imaging of myocytes expressing PKCβGFP also showed a peri-nuclear localization along with a punctate distribution pattern (Fig. 5C).

Targets for $PKC\beta_{II}$: Phosphorylation and Isoform Expression

Western analysis of PLB phosphorylation—The localization of $PKC\beta_{II}$ and functional outcomes observed in myocytes raised questions about the impact on SERCA2A and PLB expression and phosphorylation. Western analysis indicated SERCA2A and PLB expression were comparable among the 3 myocyte groups (Fig. 6A). However, a complex pattern of PLB phosphorylation emerged from these studies. Phosphorylation of Ser16 (pSer16-PLB) was not different among the 3 groups. In contrast, $PKC\beta_{II}$ up-regulation produced a significant reduction in pThr17-PLB compared to controls (Fig. 6B). Myocytes were then treated with LY for 10 min to determine whether this response was specific for PKCβ. In these studies, the reduced pThr17-PLB levels returned toward control values in $PKC\beta_{II}$-expressing myocytes, but had no influence on the pSer16-PLB level (Fig. 6C). The pThr17-PLB results are consistent with phosphatase activation by $PKC\beta_{II}$ and therefore, phosphatase inhibition should produce an outcome similar to the LY effect in $PKC\beta_{II}$-expressing myocytes. Indeed, pThr17-PLB levels were similar in control and $PKC\beta_{II}$-expressing myocytes acutely treated with the phosphatase inhibitor, calyculin A (Cal A; Fig. 6D).

Phosphorylation also was studied in myocytes labeled with ^{32}P-orthophosphate. In these studies, phosphorylation of a 6–11 kDa protein, which would coincide with PLB, was not consistently different between controls and $PKC\beta_{II}$-expressing myocytes. The lack of difference detected with radiolabeling may reflect the variable levels of pSer16-PLB detected by Western analysis. The phosphorylation results observed at Thr17 of PLB point to $PKC\beta_{II}$ modulation of protein phosphatase I, which would appear to be a common target for classical PKC isoforms (32). Phosphorylated proteins migrating at 400 and 245 kDa also were examined on radiolabeled gels because they could coincide with the ryanodine receptor and α1c subunit of the L-type Ca^{2+} channel [15,33], respectively. While phosphorylation was detected in these bands, $PKC\beta_{II}$ expression was not associated with significant changes in their phosphorylation levels compared to controls (Fig. 7A).

Additional targets—There were some significant increases in ^{32}P incorporation for other protein targets. Phosphor-imaging showed $PKC\beta_{II}$ up-regulation produced prominent increases in phosphorylation of multiple bands migrating (Fig. 7A) between 15–150 kDa. Many of these protein bands coincide with several myofilament proteins including, MLC_2 (19 kDa), cTnI (24 kDa), tropomyosin (Tm, 36 kDa), cardiac troponin T (cTnT, 41 kDa), and cardiac myosin binding protein C (cMyBP-C, 150 kDa). The phosphorylation of protein bands migrating at molecular weights comparable to MLC_2, cTnI, and cTnT were significantly increased in $PKC\beta_{II}$-expressing myocytes compared to controls (Fig. 7A).

To further explore potential targets, Western analysis with phospho-specific antibodies also was performed for cTnI and cMyBP-C. The phosphorylation pattern for cMyBP-C was complex. The most striking increase in phosphorylation was detected at Ser302 in $PKC\beta_{II}$-expressing myocytes compared to controls or myocytes expressing PKCβDN (Fig. 7B). In contrast, $PKC\beta_{II}$ expression did not significantly influence Ser273 phosphorylation, which remained nearly undetectable in all 3 groups (Fig. 7C). Phosphorylation at Ser282 tended to increase in $PKC\beta_{II}$-expressing myocytes, but did not reach statistical significance among the 3 groups (Fig. 7B). Interestingly, the enhanced phosphorylation at cMyBP-C Ser302 was not blocked by the PKCβ inhibitor, LY (Fig. 7C). Studies with the pSer23/24-cTnI Ab also verified radiolabeling results for this protein, and showed a significant increase in cTnI phosphorylation with $PKC\beta_{II}$ expression (Fig. 7D). Both 10 min and 60 min LY treatment

failed to block the enhanced cTnI phosphorylation (Fig. 7E), and the increase in pSer23/24-cTnI produced by PKCβ_{II}-expressing myocytes was maintained in the presence of CalA (Fig. 7F). Increased phosphorylation of cMyBP-C and cTnI and decreased pThr17PLB suggests PKCβ_{II} up-regulation targets multiple signaling pathways in myocytes.

A number of pathways are linked to upstream PKCβ_{II}, and yet a specific signaling pathway responsible for LY-resistant phosphorylation of downstream targets has not been described in cardiac myocytes. Phosphorylation and activation of ERK1/2 is a common PKC target (32), but ERK1/2 phosphorylation was not different in control and PKCβ-expressing myocytes (Fig 8A). A logical next step was to determine whether Ser/Thr kinases with long-term activation profiles, such as CaMKIIδ are associated with PKCβ_{II} up-regulation in adult myocytes. Indeed, this idea was supported by further work showing increases in both the expression level and phosphorylation of CaMKIIδ in myocytes expressing PKCβ_{II} compared to controls or myocytes expressing PKCβDN (Fig. 8B–E). Most importantly, CaMKIIδ phosphorylation remained elevated in response to LY (Fig. 8C,E). The Thr17-PLB and cMyBP-C are documented targets for CaMKIIδ (34,35), and the resistance to acute PKCβ inhibition by LY observed with CaMKIIδ and cMyBP-C phosphorylation in PKCβ_{II}-expressing myocytes suggests this PKC isoform may indirectly target cMyBP-C via downstream activation of CaMKIIδ. While this idea is consistent with previous work showing CaMKIIδ targets cMyBP-C, the same does not appear to be true for CaMKIIδ targeting of cTnI (36).

Thus, we pursued the alternative idea that PKCβ_{II} activates additional kinases known to target Ser23/24 in cTnI. Protein kinase A (PKA) targets this Ser cluster, but its inhibition by PKI failed to alter cTnI Ser23/24 phosphorylation in myocytes expressing PKCβ_{II} (results not shown). Protein kinase D (PKD) also targets cTnI Ser23/24 (37). In further studies, PKCβ_{II} up-regulation led to increased PKD phosphorylation (Fig. 8F,G) and LY failed to inhibit this enhanced phosphorylation (Fig. 8F,H). As with cMyBP-C, CalA treatment produced a response that was similar to LY (Fig. 8G). Overall, these analyses indicate multiple signaling pathways are activated in response to PKCβ_{II} up-regulation.

DISCUSSION

The parallel analysis of function, localization, and downstream signaling targets in the present study showed diminished shortening (Fig. 2,3) coincided with a peri-nuclear distribution pattern of PKCβ_{II} (Fig. 5) and complex changes in the phosphorylation of downstream targets (Fig. 6–8). The slowing of Ca^{2+} reuptake and contractile function (Fig. 4,6) was consistent with the reduced phosphorylation of Thr17 on PLB, and indicated PKCβ_{II} activates one or more phosphatase(s). In contrast, the increased phosphorylation of myofilament proteins, CaMKIIδ, and PKD (Fig. 7,8) and the inability of LY to acutely block their phosphorylation suggests PKCβ_{II} also modulates other targets such as myofilaments via intermediate signaling pathways. Collectively, these results indicate the documented up-regulation of PKCβ_{II} associated with human heart failure (Fig. 1; [3,8,31]) may modulate function via multiple pathways. The specific pathway(s) and functional response may depend on external neurohormones, as well as the spatial and temporal distribution of PKCβ_{II} and/or downstream signaling targets in myocytes. Thus, our results support the idea PKCβ_{II} acts as a complex mini-processor or signaling hub in adult myocytes, rather than a binary or linear signal transduction pathway [38].

Insights into animal models and failing hearts

An important goal of the present study was to determine the impact of PKCβ_{II} on contractile function in isolated myocytes. Our results provide a foundation for eventually understanding the impact of PKCβ_{II} on contractile function during heart failure, which remains

controversial [3,4,8,9,10]. In earlier animal models, there was disagreement about the influence of PKCβ_{II} up-regulation on contractile function [3,4,8,9]. Phenotypic differences among the transgenic models were attributed to developmental or load-dependent adaptations and/or alterations in gene expression [4,39]. For example, higher levels of β-MHC expression develop in transgenic mice expressing wildtype PKCβ_{II} in the myocardium [26,40]. This change alone slows myocyte shortening rate and may be responsible for decreased cardiac function in these mice [41,42]. More recently, knockout of PKCβ reduced fractional shortening when compared to controls [10]. Our results show acute PKCβ_{II} up-regulation decreased contractile function in isolated myocytes without changes in the α/β myosin heavy chain ratio, the expression of other PKC isoforms, and/or key Ca^{2+} handling proteins (Figs. 1,2,7). Moreover, decreased function developed in both rodent and rabbit myocytes (Fig. 2,3). Together, our results show PKCβ_{II} negatively modulates contractile function independent of developmental or load-induced adaptations.

While our work indicates load-dependent adaptations are not required for PKCβ_{II} modulation of contractile function, adaptations likely played an important functional role in earlier work with animal models and in human heart failure. The attenuated Ca^{2+} transient observed in the present study (Fig. 3), and lack of difference in this transient for PKCβ_{II}-expressing transgenic mice and their littermates [9] are indicative of this possibility. Direct and/or adaptive responses also could contribute to the milder hypertrophy and the shift to faster relaxation and Ca^{2+} decay rates in mice expressing constitutively active PKCβ [4,39]. Thus, the relative contribution of primary versus adaptive responses to the divergent cellular phenotypes observed in genetic models remains unclear. The relative role of these responses during chronic PKCβ_{II} up-regulation and the progression of human heart failure will require further work in animal models.

Localization of PKCβ_{II} in cardiac myocytes

An additional goal of our work was to determine the PKCβ_{II} localization pattern associated with up-regulation in myocytes. Our immunohistochemical studies demonstrated a distinct PKCβ_{II} peri-nuclear localization with a less intense punctate striated staining pattern a different pattern (Fig. 5A), which differed from earlier work. A more diffuse or cytoplasmic distribution pattern was detected in isolated neonatal myocytes [32,43] and failing and non-failing human heart sections [3]. Localization and trafficking of wild-type and constitutively active PKCβ_{II} in the myocardium of the transgenic models remains unclear. The peri-nuclear pattern detected in the present study is reminiscent of proteins localized to the rough ER and/or Golgi [44,45]. The less prominent punctate and striated distribution is consistent with the recent observation of PKCβ_{II} localization in sheep cardiac SR [46]. This SR distribution also is consistent with downstream post-translational modification of PLB (Fig. 6). The differences in localization observed here compared to earlier studies are consistent with PKCβ_{II} playing multiple roles in response to circulating neurohormones or pathophysiological conditions such as pressure overload and/or heart failure [47]. These findings also suggest localization studies may provide important clues about PKCβ_{II} trafficking, target protein localization as well as their relative role in modulating contractile function.

Ca^{2+} handling targets and their role in the functional response

The parallel measurements of contractile function and target proteins also provided a number of new insights into PKCβ_{II} modulation of contractile function. The diminished cellular shortening and slowed re-lengthening correlated well with changes in the cellular Ca^{2+} transient after PKCβ_{II} up-regulation (Fig. 3). This functional response was not associated with altered expression of SR Ca^{2+} cycling proteins (Fig. 6), and led us to focus on potential phosphorylation targets. While radiolabeling indicated similar phosphorylation

levels of PLB in controls and PKCβ$_{II}$-expressing myocytes, a more complex pattern emerged in experiments with phospho-specific antibodies. This response included LY-sensitive decreases in Thr17-PLB phosphorylation, increased Ser16-PLB and restored Thr17-PLB phosphorylation in response to CalA, and the slowing of Ca^{2+} decay with and without caffeine in PKCβ$_{II}$-expressing myocytes (Figs. 4,6). Based on these results, this PKC isoform modifies SR Ca^{2+} uptake, which is linked to phosphatase activation and a downstream reduction in Thr17-PLB phosphorylation. These observations suggest slowing of SR Ca^{2+} uptake over a longer time span and/or with sustained PKCβ$_{II}$ up-regulation at a physiological rodent heart rate is anticipated to gradually reduce Ca^{2+} loading and lead to diminished Ca^{2+} release in myocardium. The classical isoform PKCα also is expressed in myocytes, is up-regulated during heart failure [3], and up-regulation results in diminished PLB phosphorylation [2]. This decrease in PLB phosphorylation is caused by PKCα-mediated phosphorylation of inhibitor-1 (I-1) and the subsequent downstream activation of protein phosphatase I [2]. PKCβ$_{II}$ may signal via a comparable mechanism, although the failure of PKCβ$_{II}$ to modulate I-1 in neonatal myocytes [10] indicates this isoform may target alternative phosphatase(s). The possibility also remains for PKCβ$_{II}$ localization and/or signaling to adapt or change during chronic versus acute up-regulation.

The increased radiolabeling of additional protein bands in the present study indicated PKCβ$_{II}$ up-regulation may target other proteins involved in Ca^{2+} handling and/or contractile function. In earlier work, enhanced and reduced voltage-gated Ca^{2+} currents were linked to PKCβ in cardiac myocytes [14,33]. PKC phosphorylation of two N-terminal threonine residues in the L-type Ca^{2+} channel (e.g. $Ca_v1.2$) is believed to reduce Ca^{2+} current [48], while phosphorylation at Ser1928 is associated with enhanced Ca^{2+} current [14,49]. The net effect of PKCβ$_{II}$ on channel phosphorylation and function in intact adult myocytes remains unclear. PKCβ activation also phosphorylates the ryanodine receptor (Ryr) in isolated SR preparations [15] and is usually associated with improved function [14] rather than the diminished Ca^{2+} transient observed here (Fig. 4). Increased radiolabeling of proteins migrating at molecular weights associated with Ryr (400 kDa), and the α1c (110 kDa) subunit of the Ca^{2+} channel also were not detected in our study. However, the detection of PKCβ in SR vesicles was recently shown to modify Ryr2 gating by uncoupling Ryr from Ca^{2+} regulation [46], which could play a role in the diminished Ca^{2+} transient and reduced shortening amplitude observed here (Figs. 2–4). Carter and colleagues [46] concluded PKC may phosphorylate alternative residues in Ryr. The downstream activation of intermediate signaling pathways observed in the present study also could indicate intermediate signaling pathways may play a role in modulating Ryr activity.

Our radiolabeling studies also showed PKCβ up-regulation increases the phosphorylation of protens migrating at 43 and 115 kDa (Fig. 7) and it is possible these proteins contribute to the modulation of Ca^{2+} handling. Connexin-43 migrates at 43 kDa, is a known PKC target [50] phosphorylated on multiple residues [51], and PKCβ$_{II}$ inhibitors modify CX-43 electrical conductance [52]. The enhanced radiolabeling at 115 kDa could be the Na^+/Ca^{2+} exchanger (NCX). PKC phosphorylation activates NCX in biochemical studies, and phosphorylation-independent PKC-mediated reductions in NCX activity are reported in a mouse model [53]. Alternatively, this 115 kDa band may reflect enhanced PKD phosphorylation (Fig. 8) More work is needed to identify the proteins targeted in intact cells and determine the contribution of these proteins to PKCβ$_{II}$ modulation of cardiac performance.

Myofilament and signaling pathway targets

A significant component of our work focused on myofilament protein and intermediate signaling pathways phosphorylation after PKCβ$_{II}$ up-regulation (Fig. 7,8). The increased radiolabeling of cTnI and phospho-antibody detection of Ser23/24 in cTnI in intact

myocytes (Fig. 7) are consistent with earlier results in mouse myocardium, permeabilized myocytes and recombinant cTnI studies [9,11,38,54]. Phosphorylation of Ser23/24-cTnI is expected to counteract the slowing of Ca^{2+} decay to preserve relaxation rate [21]. This ability of Ser23/24-cTnI phosphorylation to accelerate relaxation helps to explain the proportionally larger slowing of Ca^{2+} decay compared to re-lengthening rate (Fig. 4). There also is mass spectrometry (MS) evidence $PKC\beta_{II}$ phosphorylates Thr144 and Ser45 in cTnI (rat sequence) [54,55], although detection of these phosphorylated residues is more variable [11,54]. Phosphorylation of Thr144 likely serves a functional role similar to Ser23/24 [5,56–58], while Ser45 phosphorylation would be expected to contribute to the contractile deficit observed here (Figs. 2,3).

In addition to cTnI, phosphorylation of myofilament MLC_2, cTnT, and cMyBP-C increased in response to PKCβ up-regulation (Fig. 7). Earlier, $PKC\beta_{II}$ phosphorylated these targets in purified myofilaments [54] and a $PKC\beta_{II}$ mouse model [39]. The specific residue $PKC\beta_{II}$ phosphorylates on cTnT is not established, but previous work showed PKCα targeted residue Thr206 in permeabilized papillary muscles and contributed to a loss of function [59]. MLC_2 phosphorylation more likely aids in adaptive processes to preserve function [60]. The intense phosphorylation of cMyBP-C Ser302 in response to $PKC\beta_{II}$ up-regulation is very similar to the phosphorylation produced by PKD [23]. This cMyBP-C Ser302 phosphorylation is associated with accelerated crossbridge cycling [23], which would counteract the diminished shortening observed here. More importantly, the similarity between cMyBP-C Ser302 phosphorylation observed in Fig. 7 and the response to PKD [23] raises the possibility $PKC\beta_{II}$ targets intermediate kinases to modify contractile performance in the adult myocyte. Our studies showing acute LY is unable to inhibit or block the phosphorylation of cTnI and MyBP-C (Fig. 7) provided further evidence intermediate signaling pathways may be activated in response to $PKC\beta_{II}$ up-regulation.

The phosphorylation of CaMKIIδ and PKD indicated $PKC\beta_{II}$ could also signal via these two kinase pathways (Fig. 8). Increased expression, phosphorylation and activity of CaMKIIδ develops during human and animal models of heart failure [61]. The diminished Ca^{2+} transient and shortening amplitudes observed in our work are consistent with enhanced $CaMKII\delta_c$ activity. However, other responses such as Ca^{2+} release in response to caffeine, Thr17-PLB phosphorylation, and the SERCA/PLB ratio were not similar to the phenotype produced by $CaMKII\delta_c$ up-regulation [62], and our understanding of proteins targeted for phosphorylation by CaMKIIδ and enzyme localization differ from the phenotype observed here [63]. Instead, the phosphorylation and functional results observed in the present study are more consistent with increased PKD activity [23,37,64]. Prolonged PKC activation results in sustained PKD auto-phosphorylation independent of PKC activity [64] which would explain the inability of LY to acutely inhibit $PKC\beta_{II}$ (Fig. 8) and yet similar functional outcomes are observed in control and PKCβDN-expressing myocytes. In addition, PKD phosphorylates cTnI and cMyBP-C [23,37] and the functional response shows similarities to shortening observed with sustained PKD activation in cardiac myocytes [65]. While our results implicate downstream signaling of PKD, more work is needed to understand the contribution of PKD and determine whether the PKD response is directly initiated by $PKC\beta_{II}$ or depends on additional intermediate signaling pathways.

In summary, our results indicate acute $PKC\beta_{II}$ up-regulation modulates contractile function via a complex set of downstream targets, which include activation of phosphatase(s) and intermediate signaling pathways, which ultimately modulate the phosphorylation state of a number of Ca^{2+} handling and myofilament targets. The picture emerging for this work strongly supports $PKC\beta_{II}$ acting as a mini-processor or hub within cardiac myocytes. Additional work is needed to identify additional phosphorylated targets detected by radiolabeling (Fig. 7). Future studies on the temporal and spatial trafficking of $PKC\beta_{II}$ and

its downstream targets will be critical for understanding the impact of chronic PKCβ_{II} up-regulation on cardiac performance.

Supplementary Material

Refer to Web version on PubMed Central for supplementary material.

Acknowledgments

We wish to thank Don Bers and Sivaramakrishnan Sivaraj for helpful discussions during the preparation of this manuscript. Immunohistochemical studies utilized the University of Michigan Morphology and Imaging core of the Michigan Diabetes Research and Training Center funded by NIH5P60 DK20572 from the National Institute of Diabetes & Digestive & Kidney Diseases. This work was supported by grants from the National Institutes of Health (HL067254 and HL089093 to MVW).

Abbreviations

ANOVA	Analysis of variance
Ab	antibody
AU	arbitrary units
BSA	bovine serum albumin
CalA	calyculin A
CaMKIIδ	Ca^{2+}-mediated calmodulin-dependent kinase IIδ
pCaMKIIδ	phospho-CaMKIIδ
cTnI	cardiac troponin I
cTnT	cardiac troponin T
CX-43	connexin-43
DMEM	Dulbecco's modified Eagle's medium
ERK1/2	extracellular signal regulated kinase 1 and 2
FBS	fetal bovine serum
FITC	fluorescein isothiocyanate
GFP	green fluorescent protein
JMEM	Joklik-modified minimal essential media
LY	LY379196
MOI	multiplicity of infection
cMyBP-C	cardiac myosin binding protein C
MHC	myosin heavy chain
MLC_2	myosin light chain 2
NCX	Na^+/Ca^{2+} exchange
P/S	penicillin and streptomycin
PLB	phospholamban
PKC	protein kinase C
PKCβDN	dominant negative protein kinase Cβ_{II}

SERCA2A	sarcoplasmic/endoplasmic reticulum Ca^{2+} ATPase 2A
SR	sarcoplasmic reticulum
SDS-PAGE	Sodium dodecyl sulfate polyacrylamide gel electrophoresis
SEM	standard error of the mean
TR	Texas Red
TTD	time to Ca^{2+} decay
TTP	time to peak
TTR	time to re-lengthening
VAD	ventricular assist device

REFERNCES

1. Metzger JM, Westfall MV. Covalent and noncovalent modification of thin filament action. Circ Res. 2004; 94:146–158. [PubMed: 14764650]
2. Braz JC, Gregory K, Pathak A, Zhao W, Sahin B, Klevitsky R, et al. PKC-α regulates cardiac contractility and propensity toward heart failure. Nat Med. 2004; 10:248–254. [PubMed: 14966518]
3. Bowling N, Walsh RA, Song GJ, Estridge T, Sandusky GE, Fouts RL, et al. Increased protein kinase C activity and expression of Ca^{2+}-sensitive isoforms in the failing human heart. Circulation. 1999; 99:384–391. [PubMed: 9918525]
4. Bowman JC, Steinberg SF, Jiang TR, Geenen DL, Fishman GI, Buttrick PM. Expression of protein kinase Cβ in the heart causes hypertrophy in adult mice and sudden death in neonates. J Clin Invest. 1997; 100:2189–2195. [PubMed: 9410895]
5. Pi YQ, Zhang DH, Kemnitz KR, Wang H, Walker JW. Protein kinase C and A sites on troponin I regulate myofilament Ca^{2+} sensitivity and ATPase activity in the mouse myocardium. J Physiol London. 2003; 552:845–857. [PubMed: 12923217]
6. Gu X, Bishop SP. Increased protein-kinase-C and isozyme redistribution in pressure-overload cardiac-hypertrophy in the rat. Circ Res. 1994; 75:926–931. [PubMed: 7923639]
7. Shin HG, Barnett JV, Chang P, Reddy S, Drinkwater DC, Pierson RN, et al. Molecular heterogeneity of protein kinase C expression in human ventricle. Cardiovasc Res. 2000; 48:285–299. [PubMed: 11054475]
8. Noguchi T, Hunlich M, Camp PC, Begin KJ, El Zaru M, Patten R, et al. Thin filament-based modulation of contractile performance in human heart failure. Circulation. 2004; 110:982–987. [PubMed: 15302786]
9. Takeishi Y, Chu GX, Kirkpatrick DM, Li ZL, Wakasaki H, Kranias EG, et al. In vivo phosphorylation of cardiac troponin I by protein kinase C β_2 decreases cardiomyocyte calcium responsiveness and contractility in transgenic mouse hearts. J Clin Invest. 1998; 102:72–78. [PubMed: 9649559]
10. Liu Q, Chen X, MacDonnell SM, Kranias EG, Lorenz JN, Leitges M, et al. Protein kinase Cα, but not PKCβ or PKCγ regulates contractility and heart failure susceptibility. Circ Res. 2009; 105:194–200. [PubMed: 19556521]
11. Kobayashi T, Yang X, Walker LA, Van Breemen RB, Solaro RJ. A non-equilibrium isoelectric focusing method to determine states of phosphorylation of cardiac troponin I: Identification of Ser-23 and Ser-24 as significant sites of phosphorylation by protein kinase C. J Mol Cell Cardiol. 2005; 38:213–218. [PubMed: 15623438]
12. Frank K, Kranias EG. Phospholamban and cardiac contractility. Ann Med. 2000; 32:572–578. [PubMed: 11127935]
13. Koide Y, Tamura K, Suzuki A, Kitamura K, Yokoyama K, Hashimoto T, et al. Differential induction of protein kinase C isoforms at the cardiac hypertrophy stage and congestive heart failure stage in Dahl salt-sensitive rats. Hyperten Res. 2003; 26:421–426.

14. Alden KJ, Goldspink PH, Ruch SW, Buttrick PM, Garcia J. Enhancement of L-type Ca^{2+} current from neonatal mouse ventricular myocytes by constitutively active PKC-β_{II}. Am J Physiol. 2002; 282:C768–C774.
15. Allen BG, Katz S. Phosphorylation of cardiac junctional and free sarcoplasmic reticulum by PKCα, PKCβ, PKA and the Ca^{2+}/calmodulin-dependent protein kinase. Mol Cell Biochem. 1996; 155:91–103. [PubMed: 8700163]
16. Noland TA, Kuo JF. Protein kinase C phosphorylation of cardiac troponin I and troponin T inhibits Ca^{2+}-stimulated MgATPase activity in reconstituted actomyosin and isolated myofibrils, and decreases actin-myosin interactions. J Mol Cell Cardiol. 1993; 25:53–65. [PubMed: 8441181]
17. Ohba M, Ishino K, Kashiwagi M, Kawabe S, Chida K, Huh NH, et al. Induction of differentiation in normal human keratinocytes by adenovirus-mediated introduction of the η and δ isoforms of protein kinase C. Molec Cell Biol. 1998; 18:5199–5207. [PubMed: 9710604]
18. Ohno S, Kawasaki H, Konno Y, Inagaki M, Hidaka H, Suzuki K. A fourth type of rabbit protein kinase C. Biochem. 1988; 27:2083–2087. [PubMed: 2837282]
19. Westfall MV, Rust EM, Albayya F, Metzger JM. Adenovirus-mediated myofilament gene transfer into adult cardiac myocytes. Meth Cell Biol. 1997; 52:307–322.
20. Green JJ, Robinson DA, Wilson GE, Simpson RU, Westfall MV. Calcitriol modulation of cardic contractile performance via protein kinase C. J Mol Cell Cardiol. 2006; 41:350–359. [PubMed: 16815434]
21. Westfall MV, Lee AM, Robinson DA. Differential contribution of troponin I phosphorylation sites to the endothelin-mediated contractile response. J Biol Chem. 2005; 280:41324–41331. [PubMed: 16236710]
22. Zhang Y, Bloem LJ, Yu L, Estridge TB, Iversen PW, McDonald CE, et al. Protein kinase C β_{II} activation induces angiotensin converting enzyme expression in neonatal rat cardiomyocytes. Cardiovasc Res. 2003; 57:139–146. [PubMed: 12504823]
23. Bardswell SC, Cuello F, Rowland AJ, Sadayappan S, Robbins J, Gautel M, et al. Distinct sarcomeric substrates are responsible for protein kinase D-mediated regulation of cardiac myofilament Ca2+ sensitivity and cross-bridge cycling. J Biol Chem. 2010; 285:5674–5682. [PubMed: 20018870]
24. Rust EM, Westfall MV, Metzger JM. Stability of the contractile assembly and Ca^{2+}-activated tension in adenovirus infected adult cardiac myocytes. Mol Cell Biochem. 1998; 181:143–155. [PubMed: 9562251]
25. Westfall MV, Borton AR. Role of troponin I phosphorylation in protein kinase C-mediated enhanced contractile performance of rat myocytes. J Biol Chem. 2003; 278:33694–33700. [PubMed: 12815045]
26. Wakasaki H, Koya D, Schoen FJ, Jirousek MR, Ways DK, Hoit BD, Walsh RA, King GI. Targeted overexpression of protein kinase C β_2 isoform in myocardium causes cardiomyopathy. Proc Nat Acad Sci. 1997; 94:9320–9325. [PubMed: 9256480]
27. Goldspink PH, Montgomery DE, Walker LA, Urboniene D, McKinney RD, Geenen DL, et al. Protein kinase C ε overexpression alters myofilament properties and composition during the progression of heart failure. Circ Res. 2004; 95:424–432. [PubMed: 15242976]
28. Kang MS, Walker JW. Protein kinase C δ and ε mediate positive inotropy in adult ventricular myocytes. J Molec Cell Cardiol. 2005; 38:753–764. [PubMed: 15850569]
29. Takeishi Y, Ping P, Bolli R, Kirkpatrick DL, Hoit BD, Walsh RA. Transgenic overexpression of constitutively active protein kinase Cε causes concentric cardiac hypertrophy. Circ Res. 2000; 86:1218–1223. [PubMed: 10864911]
30. Keranen LM, Dutil EM, Newton AC. Protein kinase C is regulated in vivo by three functionally distinct phosphorylations. Curr Biol. 1995; 5:1394–1403. [PubMed: 8749392]
31. Takeishi Y, Jalili T, Hoit BD, Kirkpatrick DL, Wagoner LE, Abraham WT, et al. Alterations in Ca^{2+} cycling proteins and Gαq signaling after left ventricular assist device support in failing human hearts. Cardiovasc Res. 2000; 45:883–888. [PubMed: 10728414]
32. Braz JC, Bueno OF, De Windt LJ, Molkentin JD. PKC alpha regulates the hypertrophic growth of cardiomyocytes through extracellular signal-regulated kinase1/2 (ERK1/2). J Cell Biol. 2002; 156:905–919. [PubMed: 11864993]

33. Zhang ZH, Johnson JA, Chen L, El-Sherif N, Mochly-Rosen D, Boutjdir M. C2 region-derived peptides of p-protein kinase C regulate cardiac Ca^{2+} channels. Circ Res. 1997; 80:720–729. [PubMed: 9130453]
34. Karczewski P, Kuschel M, Baltas LG, Bartel S, Krause EG. Site-specific phosphorylation of phospholamban peptide by cyclic nucleotide- and Ca2+/Cam dependent protein kinases of cardiac sarcoplasmic retirculum. Basic Res Cardiol. 1997; 92(Supp 1):37–43. [PubMed: 9202842]
35. Hartzell HC, Glass DB. Phosphorylation of purified cardiac muscle C-protein by purified cAMP-dependent and endogenous Ca2+-calmodulin-dependent protein kinases. J Biol Chem. 1984; 259:15587–15596. [PubMed: 6549009]
36. Boontje NM, Merkus D, Zaremba R, Versteilen A, de Waard MC, Mearini G, et al. Enhanced myofilament responsiveness upon β-adrenergic stimulation in post-infarct remodeled myocardium. J Mol Cell Cardiol. 2011; 50:487–499. [PubMed: 21156182]
37. Haworth RS, Cuello F, Herron T, Franzen G, Kentish JC, Gautel M, et al. Protein kinase D is a novel modulator of cardiac troponin I phosphorylation and regulates myofilament function. Circ Res. 2004; 95:1091–1099. [PubMed: 15514163]
38. Steinberg S. Structural basis for protein kinase C isoform function. Physiol Rev. 2008; 88:1341–1378. [PubMed: 18923184]
39. Huang L, Wolska BM, Montgomery DE, Burkart EM, Buttrick PM, Solaro RJ. Increased contractility and altered Ca^{2+} transients of mouse heart myocytes conditionally expressing PKCβ. Am J Physiol. 2001; 280:C1114–C1120.
40. Kariya K, Karns LR, Simpson PC. Expression of a constitutively activated mutant of the β-isozyme of protein kinase C in cardiac myocytes stimulates the promoter of the β-myosin heavy-chain isogene. J Biol Chem. 1991; 266:10023–10026. [PubMed: 2037558]
41. Herron TJ, Devaney E, Mundada L, Arden E, Day S, Guerrero-Serna G, et al. Ca^{2+}-independent positive molecular inotropy for failing rabbit and human cardiac muscle by α-myosin motor gene transfer. FASEB J. 2009; 24:415–424. [PubMed: 19801488]
42. Tardiff JC, Hewett TE, Factor SM, Vikstrom KL, Robbins J, Leinwand LA. Expression of the β (slow)-isoform of MHC in the adult mouse heart causes dominant-negative functional effects. Am J Physiol. 2000; 278:H412–H419.
43. Disatnik MH, Buraggi G, Mochly-Rosen D. Localization of protein kinase C isoforms in cardiac myocytes. Exp Cell Res. 1994; 210:287–297. [PubMed: 8299726]
44. Lissandron V, Podini P, Pizzo P, Pozzan T. Unique characteristics of Ca^{2+} homeostasis of the trans-Golgi compartment. Proc Nat Acad Sci. 2010; 107:9198–9203. [PubMed: 20439740]
45. McFarland TP, Milstein ML, Cala SE. Rough endoplasmic reticulum to junctional sarcoplasmic reticulum trafficking of calsequestrin in adult cardiomyocytes. J Mol Cell Cardiol. 2010; 49:556–564. [PubMed: 20595002]
46. Carter S, Pitt SJ, Colyer J, Sitsapesan R. Ca^{2+}-dependent phosphorylation of RyR2 can uncouple channel gating from direct cytosolic Ca^{2+} regulation. J Membr Biol. 2011; 240:21–33. [PubMed: 21274522]
47. Jalili T, Takeishi Y, Song G, Ball NA, Howles G, Walsh RA. PKC translocation without changes in $G\alpha_q$ and PLC-β protein abundance in cardiac hypertrophy and failure. Am J Physiol. 1999; 277:H2298–H2304. [PubMed: 10600849]
48. McHugh D, Smart EM, Catterall WA. Inhibition of cardiac L-type calcium channels by protein kinase C phosphorylation of two sites in the N-terminal domain. Proc Nat Acad Sci. 2000; 97:12334–12338. [PubMed: 11035786]
49. Yang L, Liu G, Zakharov SI, Morrow JP, Rybin VO, Steinberg SF, et al. Ser1928 is a common site for Cav1.2 phosphorylation by protein kinase C isoforms. J Biol Chem. 2005; 280:207–214. [PubMed: 15509562]
50. Bowling N, Huang X, Sandusky GE, Fouts RL, Mintze K, Esterman M, et al. Protein kinase C-α and -ε modulate connexin-43 phosphorylation in human heart. J Mol Cell Cardiol. 2001; 33:789–798. [PubMed: 11273731]
51. Solan JL, Lampe PD. Connexin phoshporylation as a regulatory event linked to gap junction channel assembly. Biochim Biophys Acta. 2005; 1711:154–163. [PubMed: 15955300]

52. Hawat G, Baroudi G. Differential modulation of unapposed connexin 43 hemichannel electrical conductance by protein kinase C isoforms. Pflugers Arch. 2008; 456 519-427.
53. Zhang YH, Hancox JC. Regulation of cardiac Na^+-Ca^{2+} exchanger activity by protein kinase phosphorylation – Still a paradox? Cell Calcium. 2009; 45:1–10. [PubMed: 18614228]
54. Wang H, Grant JE, Doede CM, Sadayappan S, Robbins J, Walker JW. PKC-β_{II} sensitizes myofilaments to Ca^{2+} by phosphorylating troponin I on threonin-144. J Mol Cell Cardiol. 2006; 41:823–833. [PubMed: 17010989]
55. Ruse CI, Willard B, Jin JP, Haas T, Kinter M, Bond M. Quantitative dynamics of site-specific protein phosphorylation determined using liquid chromatography electrospray ionization mass spectrometry. Anal Chem. 2002; 74:1658–1664. [PubMed: 12033257]
56. Montgomery DE, Wolska BM, Pyle WG, Roman BB, Dowell JC, Buttrick PM, et al. α-Adrenergic response and myofilament activity in mouse hearts lacking PKC phosphorylation sites on cardiac TnI. Am J Physiol. 2002; 282:H2397–H2405.
57. Noland TA, Raynor RL, Jideama NM, Guo XD, Kazanietz MG, Blumberg PM, et al. Differential regulation of cardiac actomyosin S-1 MgATPase by protein kinase C isozyme-specific phosphorylation of specific sites in cardiac troponin I and its phosphorylation site mutants. Biochemistry. 1996; 35:14923–14931. [PubMed: 8942657]
58. Pyle WG, Sumandea MP, Solaro RJ, De Tombe PP. Troponin I serines 43/45 and regulation of cardiac myofilament function. Am J Physiol. 2002; 283:H1215–H1224.
59. Sumandea MP, Pyle WG, Kobayashi T, de Tombe PP, Solaro RJ. Identification of a functionally critical protein kinase C phosphorylation residue of cardiac troponin T. J Biol Chem. 2003; 278:35135–35144. [PubMed: 12832403]
60. Clement O, Puceat M, Walsh MP, Vassort G. Protein kinase C enhances myosin light chain kinase effects on force development and ATPase activity in rat single skinned cardiac cells. Biochem J. 1992; 285:311–318. [PubMed: 1386218]
61. Bossuyt J, Helmstadter K, Wu X, Clements-Jewery H, Haworth RS, Avkiran M, et al. Ca^{2+}/calmodulin-dependent protein kinase IIδ and protein kinase D overexpression reinforce the histone deacetylase 5 redistribution in heart failure. Circ Res. 2008; 102:695–702. [PubMed: 18218981]
62. Maier LS, Zhang T, Chen L, DeSantiago J, Brown JH, Bers DM. Transgenic CaMKIIδ$_C$ overexpression uniquely alters cardiac myocyte Ca^{2+} handling: Reduced SR Ca^{2+} load and activated SR Ca^{2+} release. Circ Res. 2003; 92:904–911. [PubMed: 12676813]
63. Mishra S, Gray CB, Miyamoto S, Bers DM, Brown JH. Location Matters: Clarifying the concept of nuclear and cytosolic CaMKII subtypes. Circ Res. 2011; 109:1354–1362. [PubMed: 21998325]
64. Sinnett-Smith J, Jacamo R, Kui R, Wang YZM, Young SH, Rey O, et al. Protein kinase D mediates mitogenic signaling by G_q-coupled receptors through protein kinase C-independent regulation of activation loop Ser744 and Ser748 phosphorylation. J Biol Chem. 2009; 284:13434–13445. [PubMed: 19289471]
65. Goodall MH, Wardlow RD II, Boldblum RR, Ziman A, Lederer WJ, Randall W, et al. Novel function of cardiac protein kinase D1 as a dynamic regulator of Ca^{2+} sensitivity of contraction. J Biol Chem. 2010; 285:41686–41700. [PubMed: 21041300]

Highlights

This study provides a detailed analysis of PKCβ_{II} modulation of cardiac myocyte contractile function

We examined the distribution of PKCβ_{II} and phosphorylation of Ca^{2+} cycling and myofilament proteins.

PKCβ_{II} signaling involves intermediate downstream phosphatase and kinase activation

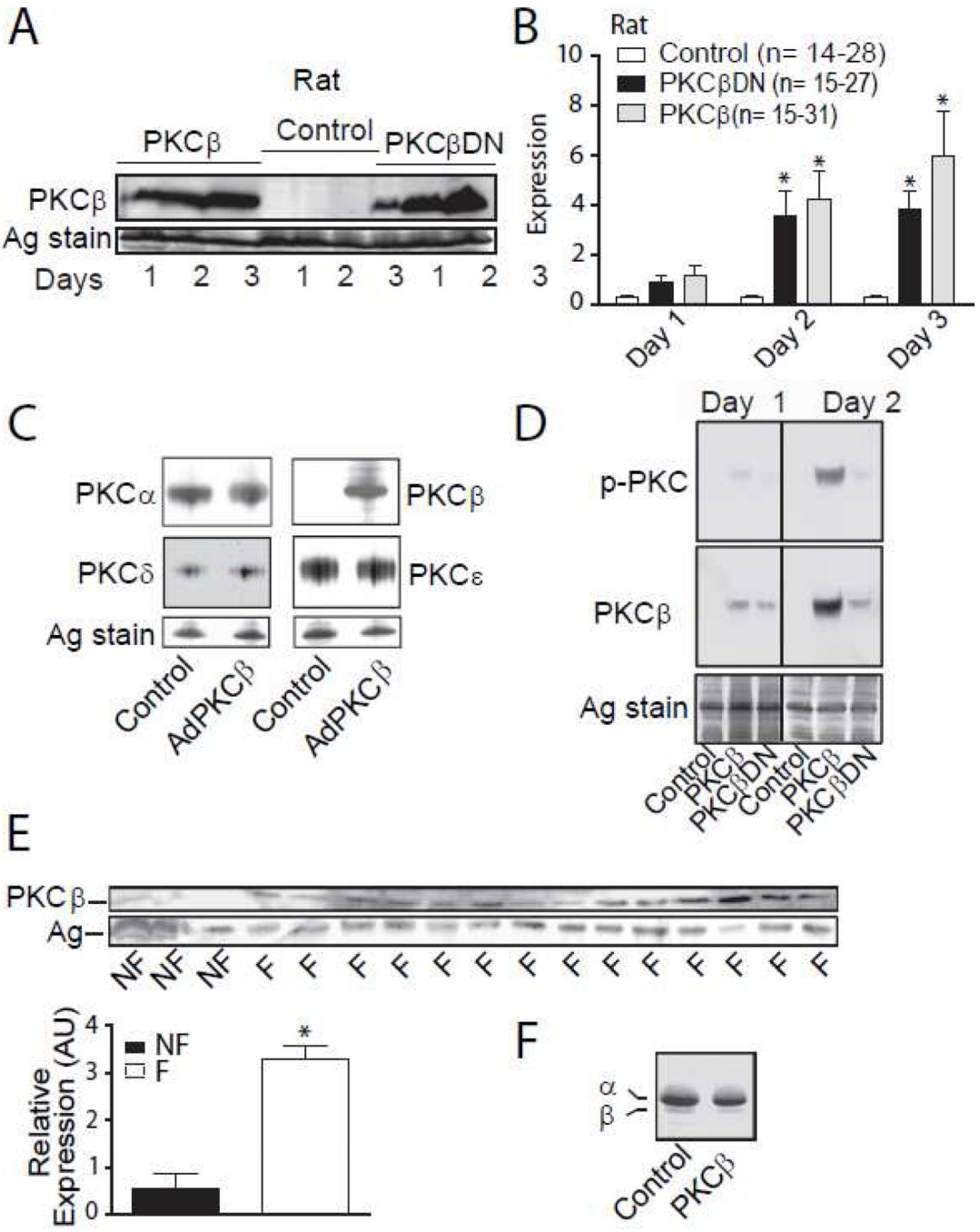

FIGURE 1.

Expression of PKC isoforms and myosin after gene transfer of PKCβ_{II} or PKCβDN (10 MOI) into rat myocytes. **A**. Representative expression of PKCβ_{II} and PKCβDN protein 1–3 days after gene transfer into adult rat myocytes. A silver-stained (Ag) portion of the SDS-PAGE gel is shown below blots in A, B, D and E to indicate protein load in each lane. **B.** Quantitative analysis of increased PKCβ_{II} and PKCβDN expression 1–3 days after gene transfer into rat myocytes. PKC expression is normalized to actin expression for each group and an asterisk indicates a statistically significant difference ($p<0.05$) compared to the control group. The number of samples analyzed for each data set is shown in the figure. **C.**

Representative expression of PKCα, PKCβ_{II}, PKCδ, and PKCε isoforms in adult rat myocytes 2 days after PKCβ_{II} gene transfer compared to time-matched control myocytes. Protein expression of PKCα, PKCδ, and PKCε remained comparable to control levels 2 days after gene transfer (see Table 1). **D**. Representative detection of the increased PKCβ phosphorylation after gene transfer of PKCβ_{II}, and the negligible phosphorylation detected in time-matched controls and myocytes expressing PKCβDN. **E**. PKCβ_{II} up-regulation in failing (F) compared to non-failing (NF) human heart tissue. Total homogenate protein loaded into each lane was 40 μg for the first two NF samples and 10 μg protein for the third NF sample and all F samples (upper panel). Proteins were separated by 12% SDS-PAGE, transferred onto PVDF and probed for PKCβ_{II}. Quantitative analysis and significant up-regulation of PKCβ_{II} in failing versus non-failing human hearts is shown in the lower panel. **F.** Representative myosin heavy chain (MHC) isoform expression resolved with 8% SDS-PAGE in adult rat myocytes.

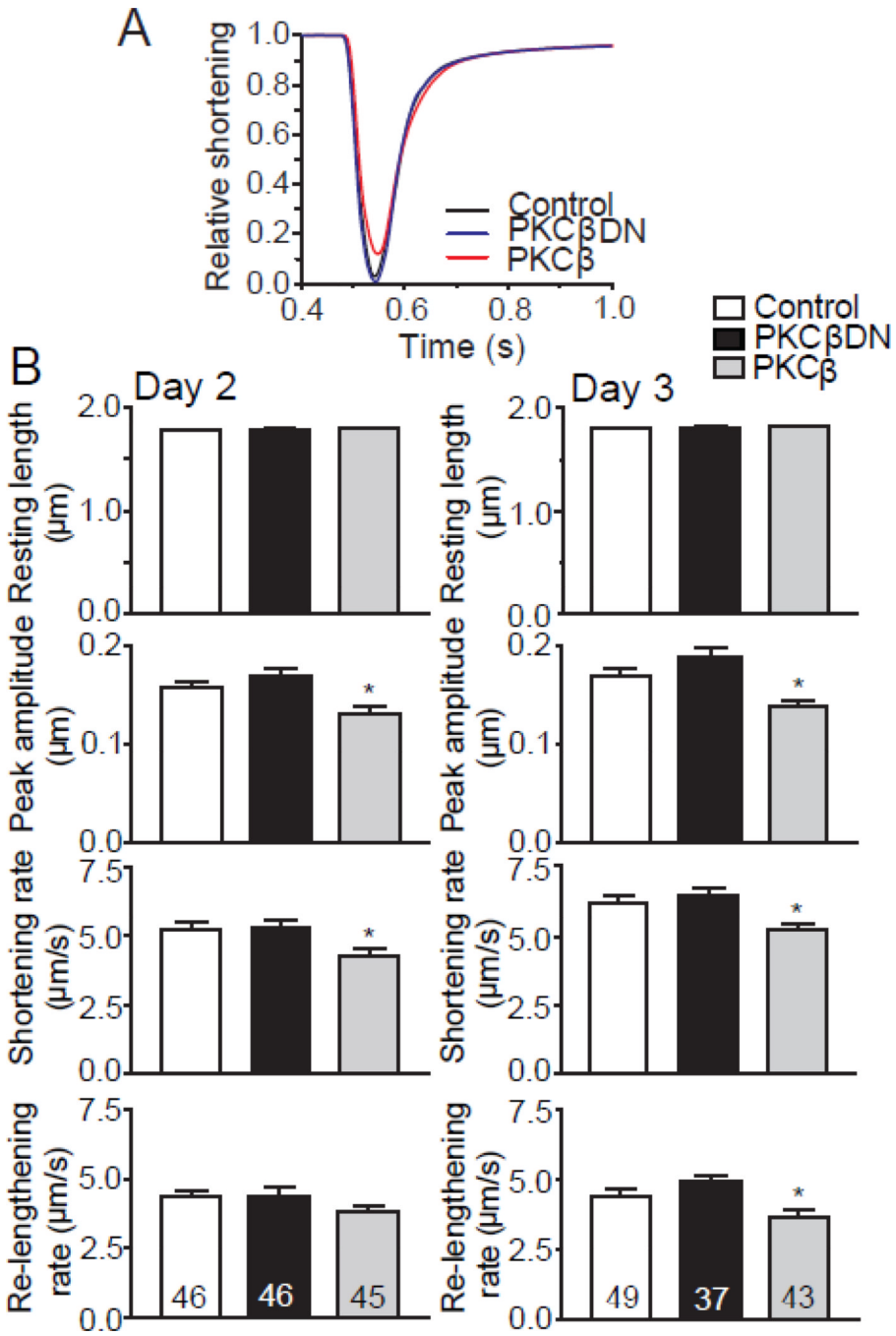

FIGURE 2.

Rat cardiac myocyte contractile function 2 and 3 days after $PKC\beta_{II}$ or PKCβDN gene transfer compared to controls. **A.** Composite shortening traces collected from control myocytes (n=46 myocytes; black), and myocytes expressing $PKC\beta_{II}$ (n=46; red) or PKCβDN (n=45; blue) 2 days after gene transfer. **B.** A comparison of contractile function in isolated rat cardiac myocytes 2 (**left panel**) and 3 (**right panel**) days after gene transfer. The number of cells analyzed for each group is shown at the bottom of each bar in the re-lengthening rate panels. Peak shortening amplitude and the rate of shortening were significantly reduced in myocytes expressing $PKC\beta_{II}$ compared to controls both 2 and 3

days post-gene transfer (*$p<0.05$). While there were no significant changes in resting sarcomere length or re-lengthening rate among the 3 groups of myocytes by 2 days, there was a significant slowing of re-lengthening rate 3 days after gene transfer in myocytes expressing $PKC\beta_{II}$ compared to controls. Measurements at both 2 and 3 days after gene transfer were not different in myocytes expressing PKCβDN compared to controls.

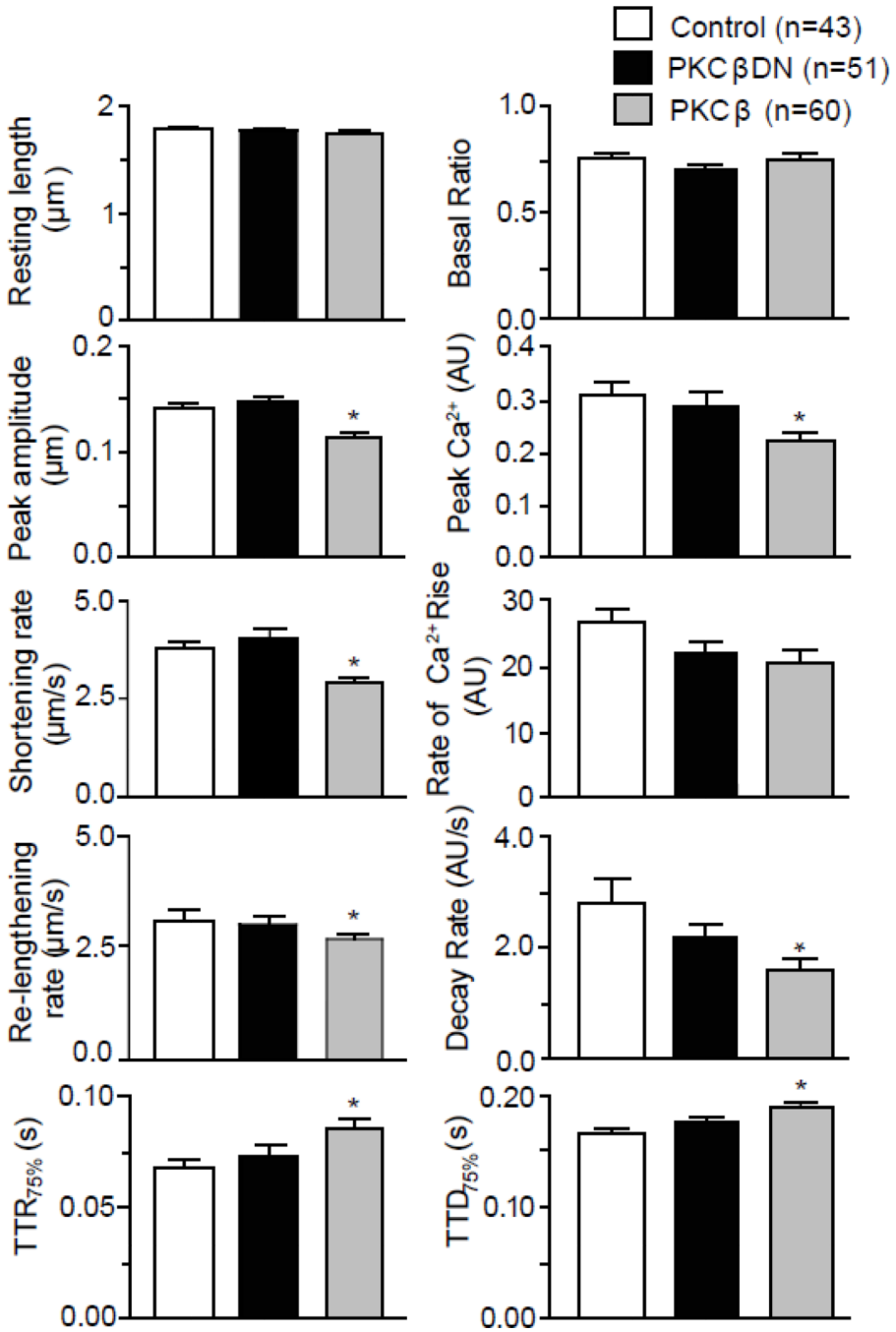

FIGURE 3.

Analysis of sarcomere shortening (left panel) and the Ca^{2+} transient (right panel) in Fura-2AM loaded rat myocytes 2 days after gene transfer. Basal and peak amplitude of shortening, the rates of shortening and re-lengthening, rates of Ca^{2+} rise and Ca^{2+} decay, and the time to 75% re-lengthening ($TTR_{75\%}$) and time to 75% Ca^{2+} decay ($TTD_{75\%}$) are shown for each group. Decreases in shortening amplitude and re-lengthening rate (*$p<0.05$) in PKCβ-expressing myocytes developed in parallel with diminished Ca^{2+} amplitude and slowing of the Ca^{2+} decay rate compared to control values. These values were not different in PKCβDN-expressing and control myocytes ($p>0.05$). The rate of shortening also slowed

in PKCβ_{II}-expressing myocytes, although the corresponding rate of Ca^{2+} rise was not significantly different in control and PKCβ_{II}-expressing myocytes.

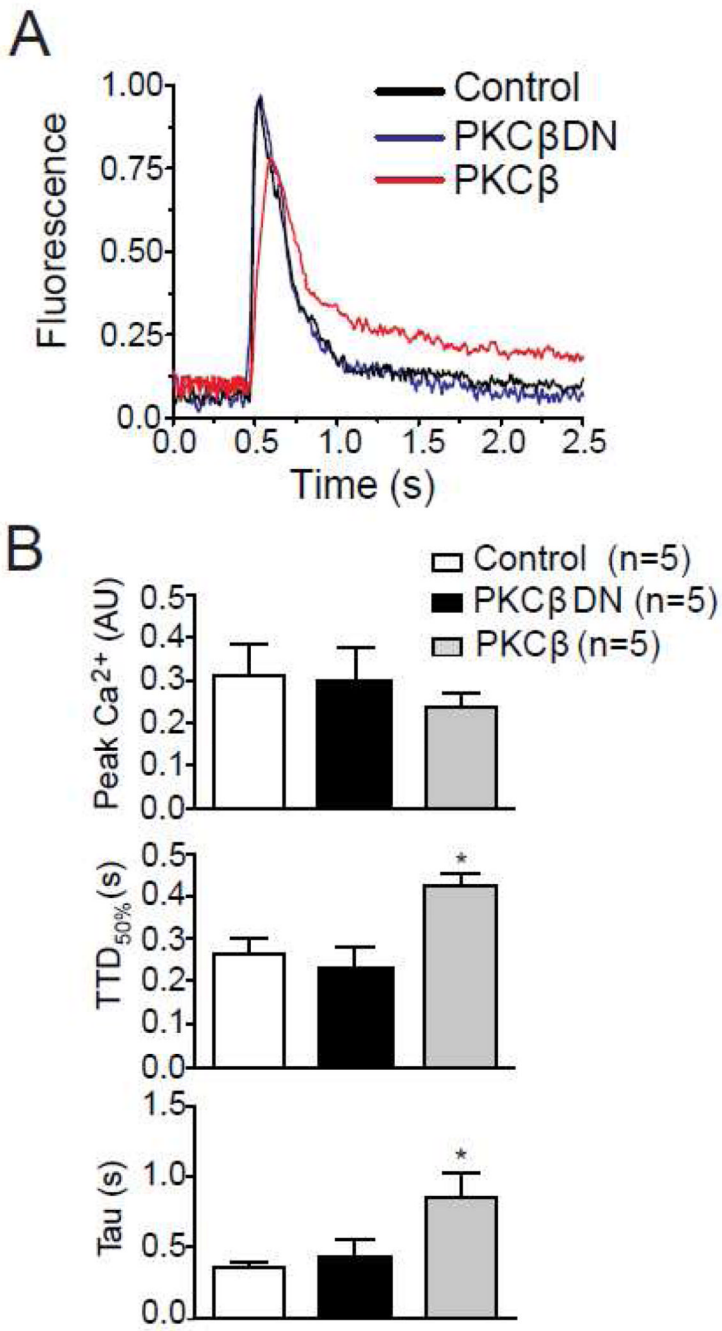

FIGURE 4.

Caffeine-induced Ca^{2+} release and re-uptake in control, $PKC\beta_{II}$- and PKCβDN-expressing adult rat myocytes. **A**. Composite caffeine-induced Ca^{2+} transients recorded in Fura-2AM-loaded myocytes expressing PKCβDN (blue), $PKC\beta_{II}$ (red), and control myocytes (black) 3 days after gene transfer. **B**. Analysis of caffeine-induced Ca^{2+} release and re-uptake in the 3 groups of myocytes. Peak Ca^{2+}, basal Ca^{2+}, and Ca^{2+} release rate (results not shown) were not significantly different between groups. All indices of Ca^{2+} re-uptake (decay rate, tau, $TTD_{50\%}$ and $TTD_{75\%}$) slowed significantly (*$p<0.05$) in myocytes expressing $PKC\beta_{II}$, compared to PKCβDN- and control myocytes.

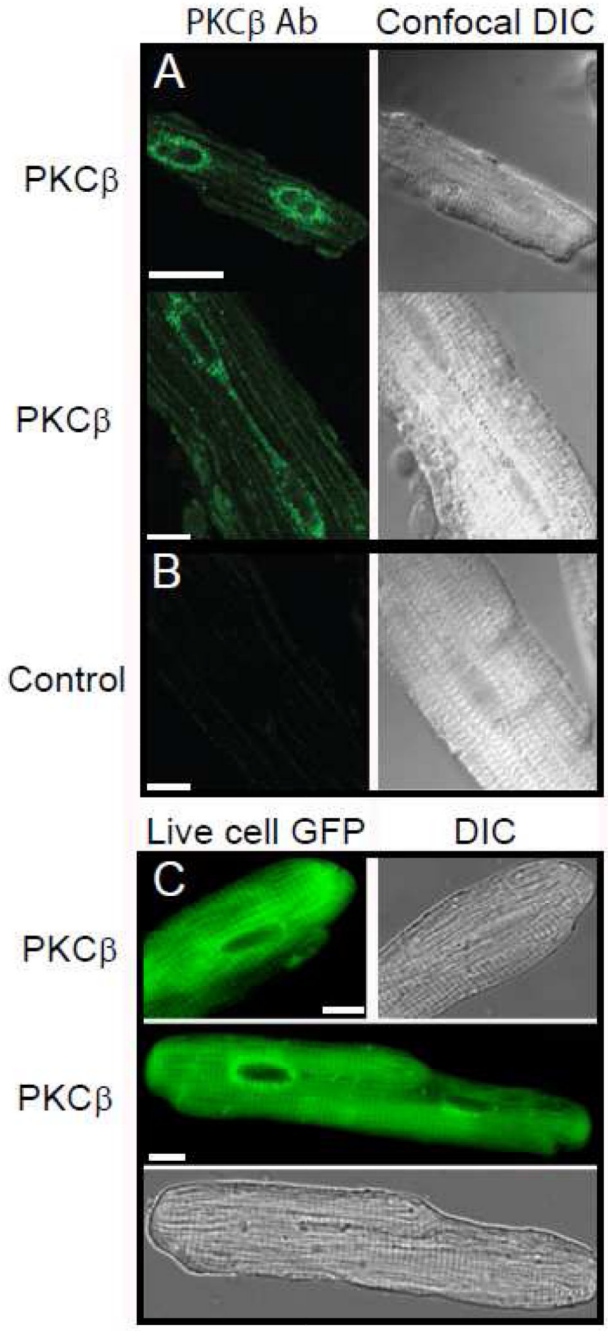

FIGURE 5.

Representative immunohistochemical labeling of PKCβ (left panels) and differential interference contrast (DIC; right panels) imaging of adult rat cardiac myocytes 2 days post-gene transfer. Myocytes were immunostained with anti-PKCβ antibody (Ab; 1:400) and FITC-conjugated goat anti-mouse secondary Ab (1:1000). **A.** The perinuclear distribution pattern of $PKC\beta_{II}$ observed in myocytes (left panels) is shown in these representative images. Scale bar in top panel equals 25 μm and 10 μm in lower panel. **B.** A representative control myocyte showing an absence of PKCβ protein detection at 2 days. Scale bar = 10 μm. Results in **C** show the perinuclear along with striated distribution detected with live cell imaging in myocytes expressing PKCβGFP. Scale bar equals 10 μm in both panels.

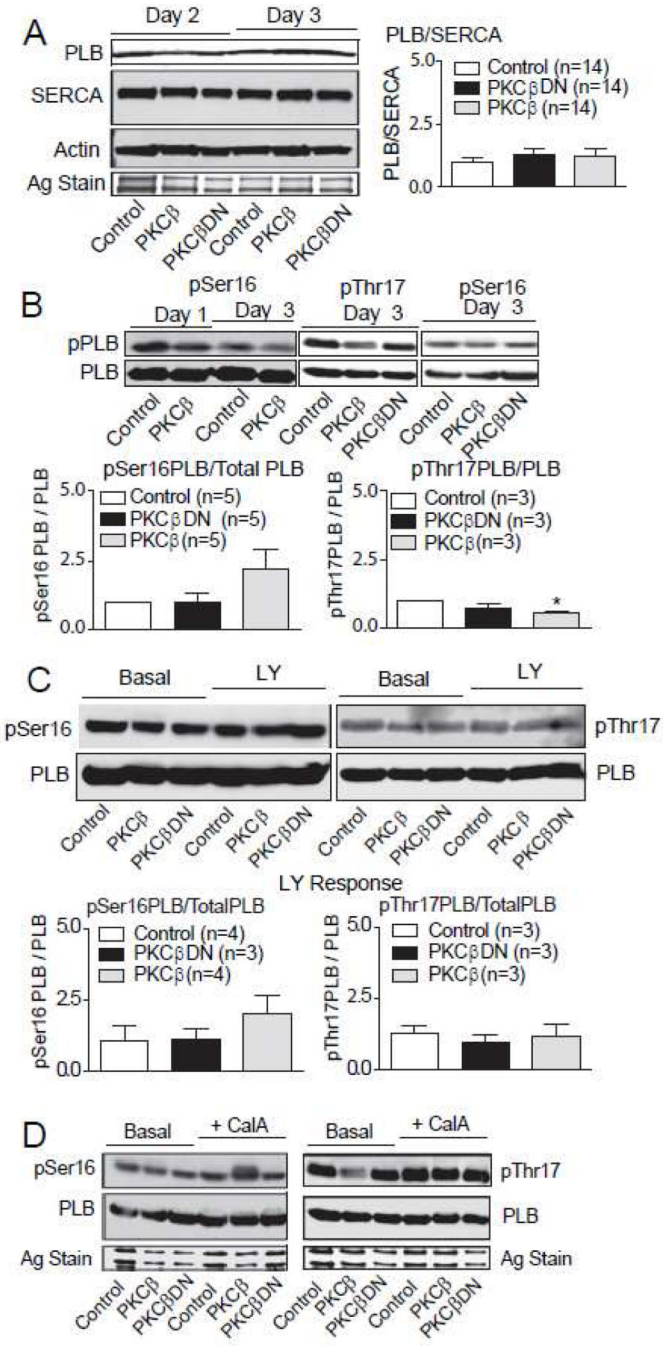

FIGURE 6.

Analysis of sarcoplasmic/endoplasmic reticulum Ca^{2+} ATPase 2A (SERCA) and phospholamban (PLB) expression and phosphorylation in control, $PKC\beta_{II}$ and PKCβDN-expressing adult rat myocytes. **A**. Representative expression of SERCA, PLB, actin and a silver- (Ag) stained gel portion in the 3 groups of myocytes is shown in the left panel. Quantitative analysis of SERCA/PLB ratio in the right panel showed no difference among the 3 groups of myocytes. The number of samples in each group is shown in the figure legend of each quantitative analysis panel for A-C, with statistical differences from control indicated by an asterisk ($p<0.05$). **B**. **Upper panel.** Representative phosphorylation of Ser16-PLB (pSer16PLB) and Thr17-PLB (pThr17-PLB) relative to total PLB expression

one and three days after gene transfer. **Lower panel.** Quantitative analysis of Ser16 (left) and Thr17 (right) PLB phosphorylation expressed relative to total PLB. **C**. **Upper panel.** Representative blots showing pSer16-PLB (left) and pThr17-PLB (right) relative to total PLB in the absence and presence of the PKCβ inhibitor LY379196 (LY; 30 nM). **Lower panel.** Quantitative analysis of pSer16-PLB/PLB and pThr17-PLB/PLB in the presence and absence of LY379196 for 3 groups of myocytes. **D**. Representative pSer16-PLB (left panel) and pThr17-PLB (right panel) detected after incubating myocytes with and without the protein phosphatase inhibitor, calyculin A (CalA; 10 nM) in control, $PKC\beta_{II}$-, and PKCβDN-expressing myocytes. In 2 separate experiments, CalA increased pSer16-PLB and restored pThr17-PLB to baseline in myocytes expressing $PKC\beta_{II}$ compared to controls.

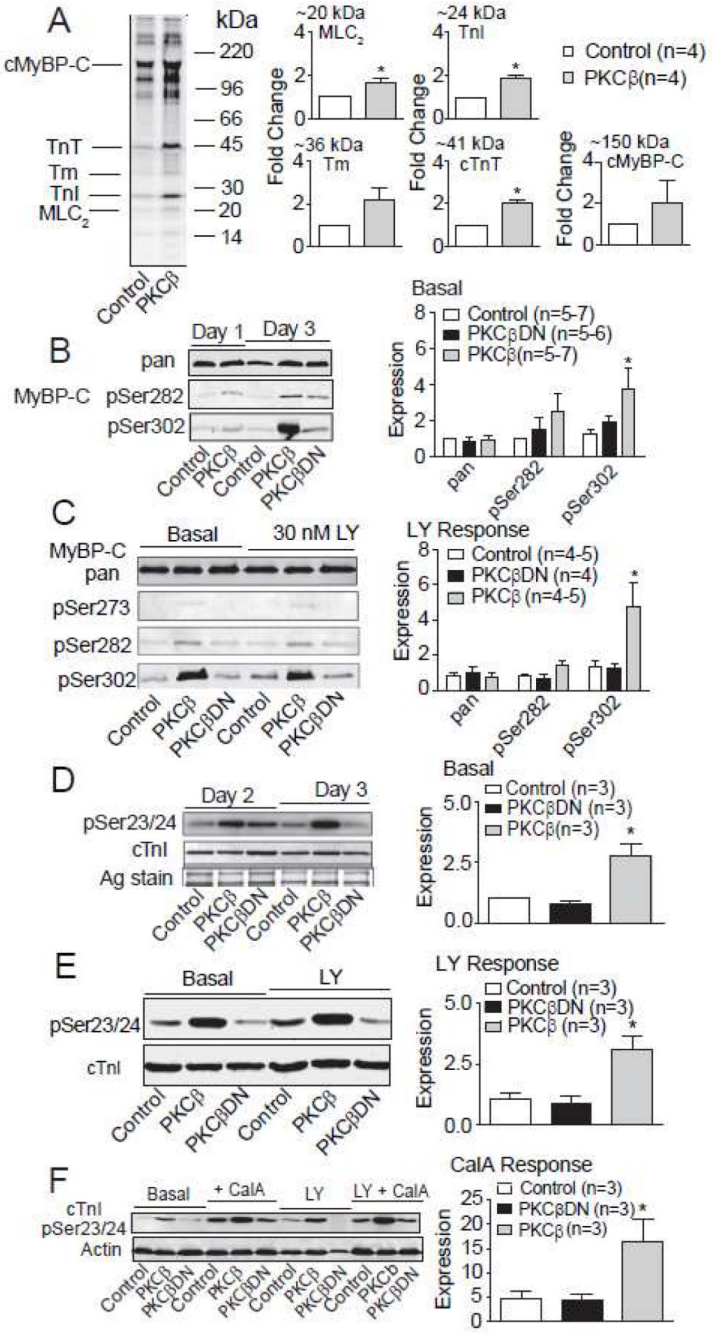

FIGURE 7.

Myofilament protein phosphorylation in response to PKCβ_{II} up-regulation in adult rat myocytes. **A. Left panel**. Representative phosphorimage showing ^{32}P-orthophosphate incorporation into proteins from control and PKC-β_{II} expressing myocytes 2 days after gene transfer. Radiolabeled proteins were separated with 12% SDS-PAGE and the quantitative analysis of phosphor-image bands (n=4 rats for each group) migrating at 20, 24, 36, 41 and 150 kDa and the myofilament protein migrating at each of these molecular weights is shown in the **right panel**. This analysis showed enhanced phosphorylation of proteins migrating at the molecular weights of myosin light chain 2 (MLC_2), cardiac troponin T (cTnT), and

cardiac troponin I (cTnI) in PKCβ_{II}-expressing myocytes compared to control levels. Phosphorylation of the 36 kDa and 150 kDa phosphor-image bands were not significantly different between the two groups (Student's T-test, $p>0.05$; n=4). **B**. **Left panel**. Representative Western analysis (left panel) of cardiac myosin binding protein C (cMyBP-C) expression (pan) and phosphorylation of Ser282 (pS282) and Ser302 (pS302) in control, PKCβ_{II}-, and PKCβDN-expressing myocytes 1 and 3 days after gene transfer. **Right panel**. Quantitative analysis indicated PKCβ_{II}-expressing myocytes showed a significant increase in pS302 compared to controls. The ratio of the phosphorylated cMyBP-C residue (pSer282; pSer302) detected relative to pan MyBP-C is normalized to day 2 controls in this pane and in the right panel of C. The number of myocyte preparations analyzed for each quantitative comparison is shown in the right panel figure legend for B-F, and asterisks indicate statistically significant differences compared to control ($p<0.05$). **C. Left panel**. Representative Westerns showing cMyBP-C protein expression (pan Ab) and phosphorylation of Ser273 (pSer273), pSer282, and pSer302 detected with phospho-specific antibodies in the absence and presence of LY379196 (LY). Detection of pSer273 was not significantly elevated above background in all groups of myocytes. **Right panel**. Quantitative analysis of pan, pSer282 and pSer302 cMyBP-C indicates LY379196 failed to inhibit enhanced pSer302 in PKCβ_{II}-expressing myocytes. **D**. **Left panel**. Representative phosphorylation detected by Western analysis of cTnI Ser23/24 (pSer23/24) after PKCβ_{II} gene transfer. **Right panel.** The ratio of pSer23/24 in cTnI relative to total cTnI is normalized to day 2 controls in this panel and in the right panel of E. Quantitative analysis indicated PKCβ_{II} expression caused an increase in cTnI pSer23/24 levels compared to controls. **E**. **Left panel.** Representative Western blot of pSer23/24 and cTnI expression in the absence and presence of Ly379196 (LY, 60 min). **Right panel**. The quantitative analysis of pSer23/24 levels in response to LY379196 indicates this PKCβ inhibitor failed to prevent or block the enhanced pSer23/24 of cTnI in PKCβ_{II}-expressing myocytes. **F. Left panel.** Representative Western blot showing pSer23/24-cTnI relative to actin in the absence and presence of CalA and LY379196 (10 min). **Right panel.** Quantitative analysis of pSer23/24-cTnI in the presence of CalA demonstrates the enhanced pSer23/24-cTnI also is preserved in the presence of the phosphatase inhibitor, CalA in PKCβ_{II}-expressing myocytes.

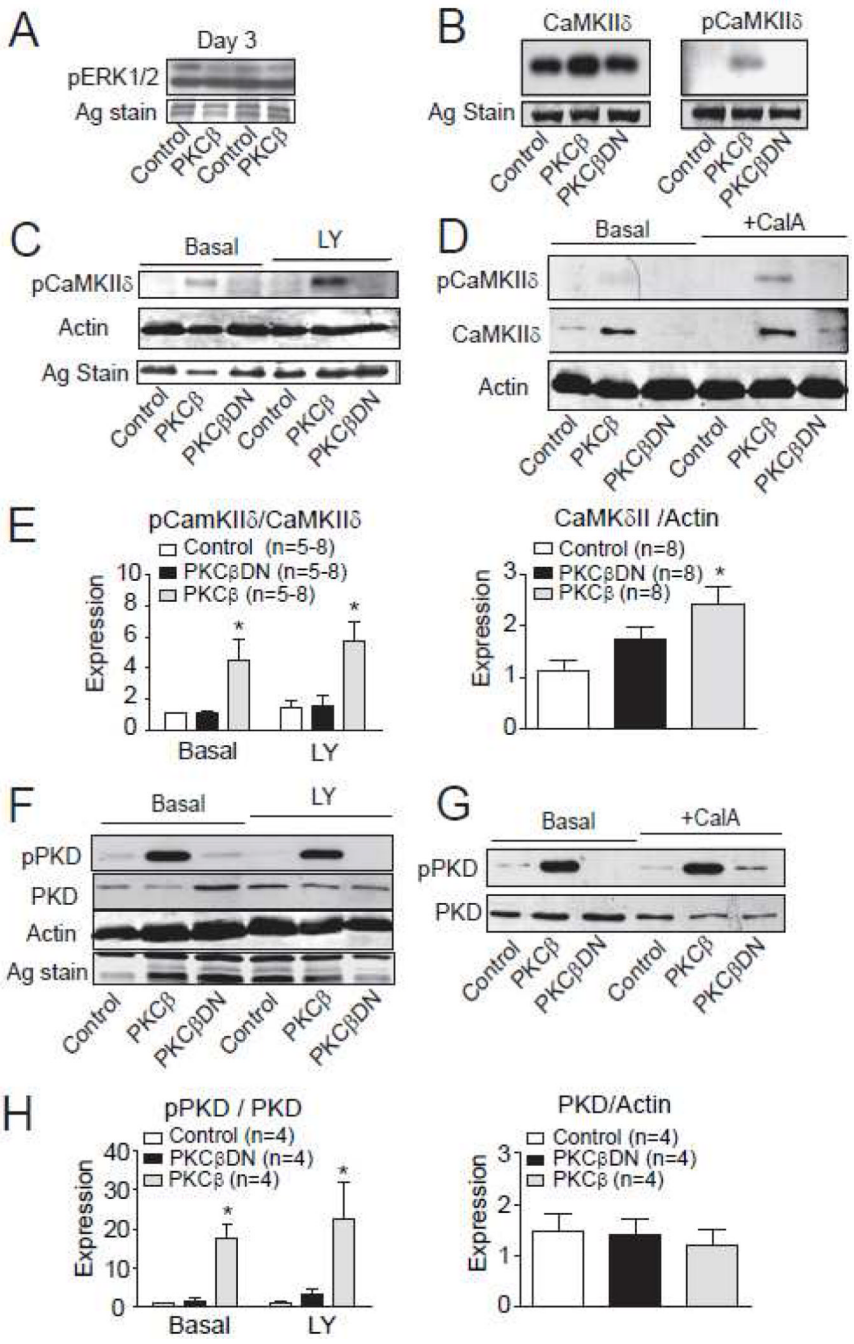

FIGURE 8.

Influence of PKCβ_{II} expression on potential downstream signaling pathways in adult rat myocytes. **A**. A representative blot showing phosphorylation of ERK1/2 (pERK1/2) in adult myocytes expressing PKCβ_{II} compared to controls. **B**. Representative Westerns showing enhanced CaMKIIδ expression (left panel) and phosphorylation of this kinase (right panel) in myocytes expressing PKCβ_{II} compared to controls and myocytes expressing PKCβDN. **C**. Western analysis indicates LY379196 (LY) fails to inhibit the enhanced CaMKIIδ phosphorylation observed in adult myocytes expressing PKCβ_{II}. Actin and an Ag-stained portion of the gel are shown to indicate the protein load in each lane. **D**. Representative blot

showing PKCβ_{II}-induced increases in CaMKIIδ phosphorylation in the absence and presence of Cal A. CaMKIIδ phosphorylation remains enhanced in the presence of CalA compared to controls and there is no difference between the PKCβDN and control groups. **E**. Quantitative analysis of PKCβ_{II}-induced increases in the ratio of phosphorylated CaMKIIδ (pCaMKIIδ) to total CaMKIIδ in the absence and presence of LY379196 (left panel). Expression of CaMKIIδ is normalized to actin in the 3 myocyte groups and is up-regulated in myocytes expressing PKCβ_{II} compared to controls(right panel). **F**. Western analysis of phospho-PKD (pPKD) and PKD indicates PKCβ_{II} expression does not acutely modify PKD expression in myocytes, but produces significantly enhanced PKD phosphorylation. In addition, the PKCβ inhibitor, LY379196 failed to inhibit or block the phosphorylation of PKD in adult myocytes expressing PKCβ_{II}. **G**. Representative Western demonstrates CalA has no influence on PKD phosphorylation in the 3 groups of myocytes. **H**. Quantitative analysis of the PKCβ_{II}-related increases in pPKD in the absence and presence of LY379196 (left panel). The right panel shows similar levels of PKD expression in control, PKCβ_{II}- and PKCβDN-expressing myocytes (right panel). Expression of pPKD is normalized to total PKD in the left panel and PKD expression is normalized to actin in the right panel. The number of experiments is indicated in the figure legend of each quantitative panel, with *$p<0.05$ considered statistically significant.

Table 1

Summary of protein expression levels of PKC isoforms normalized to a silver (Ag) stained gel band after gene transfer of PKCβ compared to time-matched control myocytes. Data was collected as relative absorbance units (AU) and results shown are mean±SEM compared with an unpaired Student's t-test

Western analysis	Control (n) (AU Western/ AU for Ag stain)	AdPKCβ_{II} (n) (AU Western/ AU for Ag stain)
PKCα	1.88±0.26(10)	2.18±0.39(10)
PKCδ	0.38±0.02 (7)	0.46±0.09 (7)
PKCε	1.54±0.47 (6)	1.64±0.61 (5)

(*$p<0.05$ versus control values; ( ) = number of hearts).